

# Temporary Satellite Capture of Short-Period Jupiter Family Comets from the Perspective of Dynamical Systems<sup>1</sup>

K. C. Howell,<sup>2</sup> B. G. Marchand,<sup>3</sup> and M. W. Lo<sup>4</sup>

## Abstract

The Temporary Satellite Capture (TSC) of short-period comets, such as Oterma and Helin-Roman-Crockett, by Jupiter has intrigued astronomers for many years. A widely accepted approach to study TSC is to numerically integrate the equations of motion for the  $n$ -body problem using a wide range of initial conditions obtained from the heliocentric *two*-body problem; then, a search ensues for instances when the Joviocentric energy becomes negative. More recently, a preliminary analysis involving the application of Dynamical Systems Theory (DST) to the Sun-Jupiter-comet *three*-body problem has provided significant insight into the motion in the Sun-Jupiter system and offered a simple model to account for the TSC phenomena observed in Jupiter family short-period comets. The accuracy of this model can be immediately verified since ephemeris data is available for comet trajectories.

## Introduction

In July 1943, L. E. Cunningham and R. N. Thomas [1] published data that revealed, among other things, that the recently discovered comet 39P/Oterma had passed close to Jupiter in 1938. Astronomers subsequently noted that the orbit of the comet was “not particularly stable” due to close approaches of Jupiter. It is a generally accepted practice in astronomy to explain the erratic behavior of short-period comets such as Oterma in the context of a heliocentric *two*-body problem where perturbations from the outer planets result in significant changes to the orbital parameters of a given comet. However, evaluating this issue from the perspective of Dynamical Systems Theory (DST) has offered new insight into the erratic dynamical behavior of this and other comets.

<sup>1</sup>An earlier version of this paper was presented as paper AAS-00-155 at the AAS/AIAA Space Flight Mechanics Meeting, Clearwater, Florida, January 23-26, 2000.

<sup>2</sup>Professor, School of Aeronautics and Astronautics, Purdue University, West Lafayette, Indiana 47907.

<sup>3</sup>Graduate Student, School of Aeronautics and Astronautics, Purdue University, West Lafayette, Indiana 47907.

<sup>4</sup>Member of Technical Staff, Jet Propulsion Laboratory, California Institute of Technology, Pasadena, California.

Comets like 39P/Oterma (OTR) and 111P/Helin-Roman-Crockett (HRC) are classified as Jupiter family short-period comets. These comets share at least one significant orbital characteristic: at some time during their dynamical evolution each experiences a low-velocity close encounter with Jupiter such that the Joviocentric energy becomes negative. This event is denoted as Temporary Satellite Capture (TSC). Kazimirchak-Polonskaya [2] studied TSC in the early 1970's by numerically integrating the orbits of a group of minor bodies, with a wide range of heliocentric orbital elements as initial conditions. She used an  $n$ -body integrator to propagate the initial conditions and searched for instances when the bodies crossed the sphere of influence of Jupiter, Saturn, Uranus, or Neptune. This effort was an attempt to create the dynamical circumstances required for a TSC to occur and thus establish a criterion for capture. Carusi [3–10], in collaboration with Pozzi [3], Valsecchi, [4–10], Kresák [7, 9], and Perozzi [8, 9], employed a similar approach to study the capture phenomena.

Investigations of this problem have subsequently continued. In the mid-1970's, Horedt [11], Heppenheimer [12–13], and Porco [13] considered the problem of TSC in the context of the planar circular restricted *three*-body problem (CR3BP). These authors attributed the strange behavior of some Jupiter family comets to the separatrices associated with the libration point  $L_1$  in the Sun-Jupiter system. Though not explicitly stated, this may be the first study linking the behavior of short-period Jupiter family comets to the dynamical structure associated with the collinear libration points in the Sun-Jupiter system. In a more recent effort, Lo and Ross [14] suggested that the chaotic nature of the dynamics of Jupiter family short-period comets can be explained in the context of the stable and unstable manifolds associated with the collinear libration points  $L_1$  and  $L_2$  in the Sun-Jupiter *three*-body system. This approach successfully reveals many of the significant features of the motion of these comets. It is also noted, however, that certain comet behavior is even more completely reflected in the evolution of stable and unstable manifolds corresponding to the periodic orbits in the vicinity of  $L_1$  and  $L_2$ . Koon, Lo, Marsden, and Ross [15] considered this issue in the context of the planar restricted *three*-body problem and presented some theoretical results as well. But, to allow for a more thorough investigation of the critical features in the context of periodic orbits and quasi-periodic trajectories in the three-dimensional *three*-body problem (3BP), the complexities involved with the out-of-plane component of the motion are required; such analysis is the focus of the current effort.

In this investigation, the motion of OTR and HRC are considered within the framework of the three-dimensional, restricted *three*-body problem. This formulation allows for consideration of the impact of the stable and unstable manifolds, associated with both halo orbits and Lissajous trajectories, on the evolution of the comet trajectories. In particular, the problem is posed as a search for trajectory arcs along the stable and/or unstable manifolds that reflect the comet orbit. Initially, the comet trajectories are viewed in the context of the circular (but three-dimensional) restricted problem. The inherent symmetries of this model simplify the task of locating a trajectory arc that closely matches a segment along the path of OTR and HRC, particularly during TSC. Such a trajectory arc is defined as a "match." Once a match is identified, the solution is transferred to the ephemeris model. In this model, actual ephemeris data for the motion of the primary bodies is used during the numerical integration of the relative equations of motion. The purpose of this last step is to improve the accuracy of the match. Of course, the final arc that is

computed is evaluated against the actual comet path that is also available from ephemeris information.

## Background

### *Circular Restricted Three-Body Problem*

In the simplified Sun-Jupiter-comet system, it is assumed that the mass of the comet is both constant and negligible, relative to the two larger primaries. It is also initially assumed that the motion of the primaries about the barycenter of the system is circular. Typically, the motion of comets is considered from an inertial, heliocentric perspective. However, the more significant features of TSC are best viewed from the perspective of the Sun-Jupiter rotating frame. Let the Sun-Jupiter rotating frame be defined such that the  $x$ -axis is directed from the Sun towards Jupiter. Then, the  $z$ -axis is normal to the invariant plane of motion of the primaries, in the direction of orbital angular momentum, and the  $y$ -axis completes the right-handed triad.

By modeling the comet as an infinitesimal particle in a *three*-body system, the initial search for a match is confined to the three-dimensional solution space of the CR3BP. Thus, any potential motion of a comet in this regime is based on an understanding of this available solution space. Of course, with no general solution for motion in the restricted *three*-body problem, any analysis of the behavior begins with a consideration of particular solutions. For this investigation, such solutions include the five equilibrium, or libration, points  $L_i$  as well as fundamental motions in the vicinity of the collinear libration points  $L_i$  ( $i = 1, 2, 3$ ), such as periodic orbits. Viewed in the Sun-Jupiter rotating frame, it is clear that the paths of OTR and HRC are neither periodic nor stationary. On the contrary, their evolution appears chaotic in nature. However, equilibrium and periodic solutions provide the structure necessary to identify and numerically produce trajectory arcs in the CR3BP that resemble the observed paths of these comets, specifically by examining the flow toward and away from such solutions. Naturally, there are an infinite number of periodic solutions that satisfy the equations of motion of this system. Families of halo orbits in the vicinity of the collinear libration points are selected here as the basic framework for this analysis. Experience with such periodic orbits, as well as the associated stable and unstable manifolds, suggests behavior that is similar in nature to that observed in the motion of the comets. For notational purposes, let SJL1 denote the Sun-Jupiter  $L_1$  halo family, and SJL2 denote the Sun-Jupiter  $L_2$  halo family. These continuous, three-dimensional families are represented in Fig. 1 in terms of  $xz$ -plane projections of a limited number of periodic trajectories that are members of these families.

### *Dynamical Systems Approach*

The geometrical theory of dynamical systems (from Poincaré) is based on the phase portrait of a dynamical system as discussed in various mathematical sources [16–23]. Periodic solutions and equilibrium points are two examples of the fundamental models available for the phase space, that is, invariant manifolds. Equilibrium points and periodic orbits exist specifically in the center manifold, a significant subspace of the phase space. However, it is possible to exploit the hyperbolic nature of these types of solutions in the restricted problem, by using other invariant manifolds, that is, the associated stable and unstable manifolds, to generate

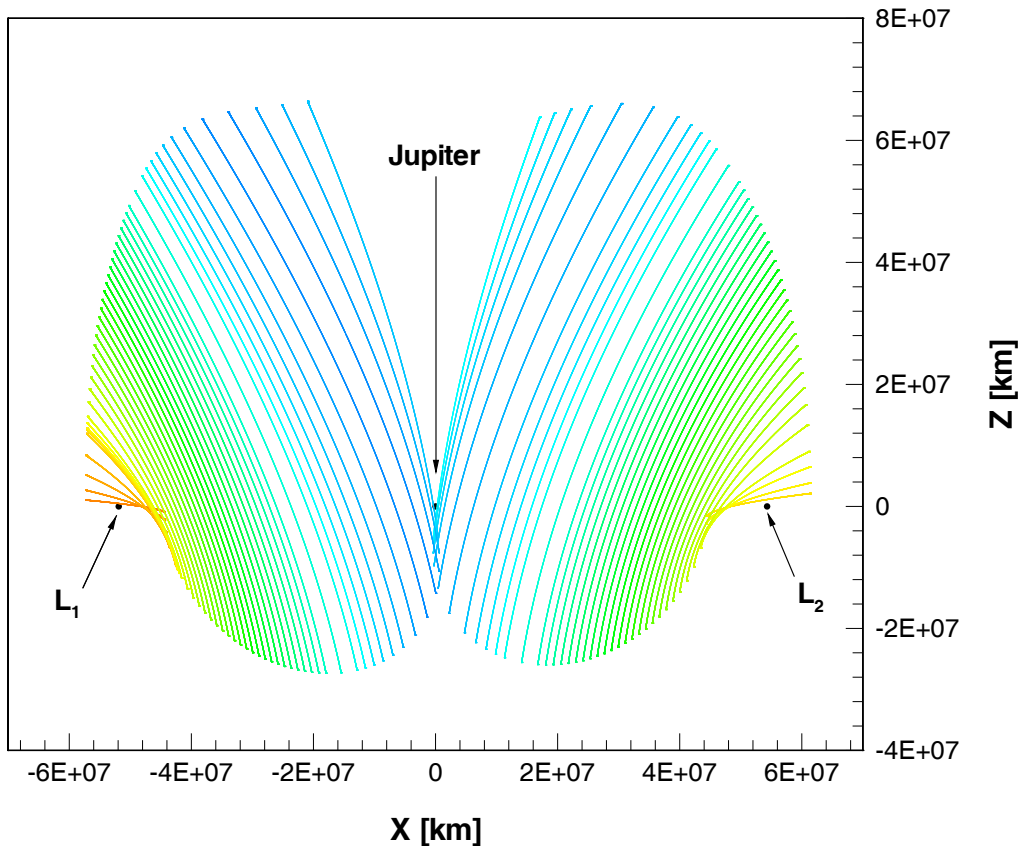


FIG. 1. Sun-Jupiter  $L_1$  and  $L_2$  Halo Families.

general trajectory arcs in this region of space. The stable and unstable manifolds asymptotically approach and depart these fundamental solutions. The first concern, then, is the computation of the stable and unstable manifolds associated with particular equilibrium points or periodic halo orbits.

As mentioned, for this investigation, periodic halo orbits are used as the reference solution for investigating the phase space. A nonlinear system and its flow give rise to a nonlinear map. Then, along a periodic orbit of the flow, any state can be defined as a fixed point for the map. Suppose that  $\mathbf{x} = \mathbf{x}_e$  is a fixed point of the map  $\mathbf{x}(t_{k+1}) = F(\mathbf{x}(t_k))$ . To investigate the behavior near the periodic solution  $\mathbf{x}(t_{k+i}) = F^i(\mathbf{x}(t_k)) = \mathbf{x}(t_k)$ , of period  $T$ , and the fixed point based at  $\mathbf{x} = \mathbf{x}_e$ , introduce a disturbance such that  $\mathbf{x} = \mathbf{x}_e + \mathbf{y}$  and, then, a discrete-time representation of the linear system,  $\mathbf{y}(t_{k+1}) = \Phi(t_{k+1}, t_k)\mathbf{y}(t_k)$ , allows for an assessment of the stability of the periodic solution. The procedure is based on the availability of the monodromy matrix associated with a particular halo orbit. As with any discrete mapping of a fixed point, the characteristics of the local geometry of the phase space can be determined from the eigenvalues and eigenvectors of the monodromy matrix (that is, the state transition matrix (STM),  $\Phi(T + t_0, t_0)$ , after one period ( $T$ ) of the motion). They are characteristic of the fixed point as well as the halo orbit itself. Once stable, unstable, and center eigenspaces are identified, a correspondence with one state on the periodic solution is established for computational purposes. Then, the eigenvector directions associated with other states along the periodic orbit can be determined by mapping these vectors using the STM. That is, if  $\hat{\mathbf{Y}}^w$  is the six-dimensional unit

stable eigenvector direction associated with the fixed point  $\mathbf{x}(t_0) = \mathbf{x}(t_0 + T) = \mathbf{x}_e$  on the periodic solution after one period of the motion ( $T$ ), then  $\hat{\mathbf{Y}}^{W_s}(t_i) = \Phi(t_i, t_0) \hat{\mathbf{Y}}^{W_s} / \|\Phi(t_i, t_0) \hat{\mathbf{Y}}^{W_s}\|$  is the unit stable direction associated with the state  $\mathbf{x}(t_i)$ .

The stable ( $E^s$ ), unstable ( $E^u$ ), and center ( $E^c$ ) eigenspaces associated with  $\mathbf{x}_e$  span the linear phase space. These three fundamental subspaces are themselves invariant sets. The three fundamental eigenspaces intersect at  $\mathbf{x}_e$  and are tangent to the local stable ( $W_{loc}^s$ ), unstable ( $W_{loc}^u$ ), and center ( $W_{loc}^c$ ) manifolds corresponding to the nonlinear map. Furthermore, since  $W_{loc}^s$  and  $W_{loc}^u$  are tangent to  $E^s$  and  $E^u$  at  $\mathbf{x}_e$ , respectively, the asymptotic nature of the solutions is preserved in the vicinity of  $\mathbf{x}_e$  for the map. Thus, the local approximation of the stable (unstable) manifold involves calculating the eigenvector associated with the stable (unstable) eigenvalue that corresponds to the fixed point  $\mathbf{x}_e$ . Hence, the global stable and unstable manifolds can be approximated numerically by propagating initial conditions that lie on  $W_{loc}^s$  and  $W_{loc}^u$ . For instance, near  $\mathbf{x}_e$ ,  $W^s$  is determined to first order, by  $\hat{\mathbf{Y}}^{W_s}$ . Remove the fixed point  $\mathbf{x}_e$  from the stable manifold to form two half-manifolds  $W^{s+}$  and  $W^{s-}$ . Consider a state  $\mathbf{x}_s$  on  $W^{s+}$ . Integrating forward and backward in time from  $\mathbf{x}_s$  produces  $W^{s+}$ . Thus, there exists some arbitrarily small constant  $d$  such that  $\mathbf{x}_s = \mathbf{x}_e + d \cdot \hat{\mathbf{Y}}^{W_s}$  lies on the local stable manifold,  $W_{loc}^s$ . Higher order expressions for  $\mathbf{x}_s$  are available but not necessary. Thus, by numerically propagating the nonlinear vector field with initial state  $\mathbf{x}_s$ , the global stable manifold,  $W^s$ , associated with  $\mathbf{x}_e$ , can be computed.

In configuration space, the collection of all trajectories that represent the stable and unstable manifolds associated with numerous states along the periodic orbit forms, locally, a three-dimensional surface. This can be further expanded to consider a large subset of a family of orbits, such as SJJ1 and SJJ2. In such a case, the collection of all stable and unstable manifolds—represented in terms of a large collection of numerically determined trajectories—that asymptotically approach and depart this subset of the family forms a volume in configuration space. The search for a match to reflect a particular comet trajectory in this regime involves the search for a trajectory arc, from among this large volume of numerical trajectories (associated with the SJJ1 and SJJ2 halo families). This arc must resemble the path of the comet particularly *in the vicinity* of Jupiter while the comet is captured. Clearly, this type of search is a nontrivial task. Nevertheless, the symmetry properties inherent in this problem are very useful in simplifying the search process for a match (that is, in narrowing the solution space of interest).

#### *Symmetry of Solutions in the CR3BP*

The form of the mathematical model for the CR3BP lends itself to various types of symmetries. The more obvious one is, of course, the  $xy$ -plane symmetry. That is, if  $[x \ y \ z \ \dot{x} \ \dot{y} \ \dot{z}]^T$  satisfies the equations of motion (EOMs) then so does  $[x \ y \ -z \ \dot{x} \ \dot{y} \ -\dot{z}]^T$ . This property leads to the existence of northern and southern families of periodic halo orbits. A northern halo family is characterized by a maximum out-of-plane excursion ( $A_z$  amplitude) that lies above the  $xy$ -plane ( $+z$ ). A southern halo family has a maximum out-of-plane excursion below the  $xy$ -plane ( $-z$ ). The term “out-of-plane” denotes the plane of motion of the primaries. The two halo families represented in Fig. 1 are both northern families of solutions. This northern/southern symmetry of solutions is defined here as symmetry property 1 (SP1). The structure of the EOMs also lends itself to time-invariance. That is, if the independent variable, time ( $t$ ), is transformed to  $\tau = -t$  it is clear that, if

$[x \ y \ z \ \dot{x} \ \dot{y} \ \dot{z}]^T$  satisfies the EOM's for  $\Delta t > 0$ , then  $[x \ -y \ z \ -\dot{x} \ \dot{y} \ -\dot{z}]^T$  also satisfies the EOM's for  $\Delta t < 0$ . The symmetry due to time invariance is defined here as symmetry property 2 (SP2). These two symmetries, SP1 and SP2, simplify the task of characterizing the solution space. This task is further simplified by identifying the surfaces of zero-velocity and, thus, regions that are excluded for motion in the CR3BP.

#### *Zero-Velocity Surfaces and Regions of Exclusion*

In the CR3BP, propagation of a set of initial conditions will result in a path that is bounded by the zero-velocity surfaces, as discussed by Szebehely [24]. For a given value of the pseudo-energy, it is well-known that these zero-velocity surfaces bound the regions that represent the available solution space and thus, by default, also indicate regions that are excluded as the path of the third body (comet or particle) evolves. The Sun-Jupiter  $L_1$  and  $L_2$  halo families, that is, those depicted in Fig. 1, correspond to a specific range of values of the Jacobi Constant. The associated zero-velocity surfaces then apportion the configuration space into three regions of motion: the interior region, the exterior region, and the temporary satellite capture (TSC) region. A comet moving within the interior region is in an orbit contained within the heliocentric orbit of Jupiter. A comet moving in the exterior region is in an orbit that extends beyond the heliocentric orbit of Jupiter. A comet that shifts into the TSC region is temporarily captured by Jupiter and, thus, remains in the vicinity of the planet until it escapes and crosses into either the interior or exterior region. To better visualize these three regions consider the zero-velocity surface, illustrated in Fig. 2, associated with a Jacobi Constant that possesses a value of

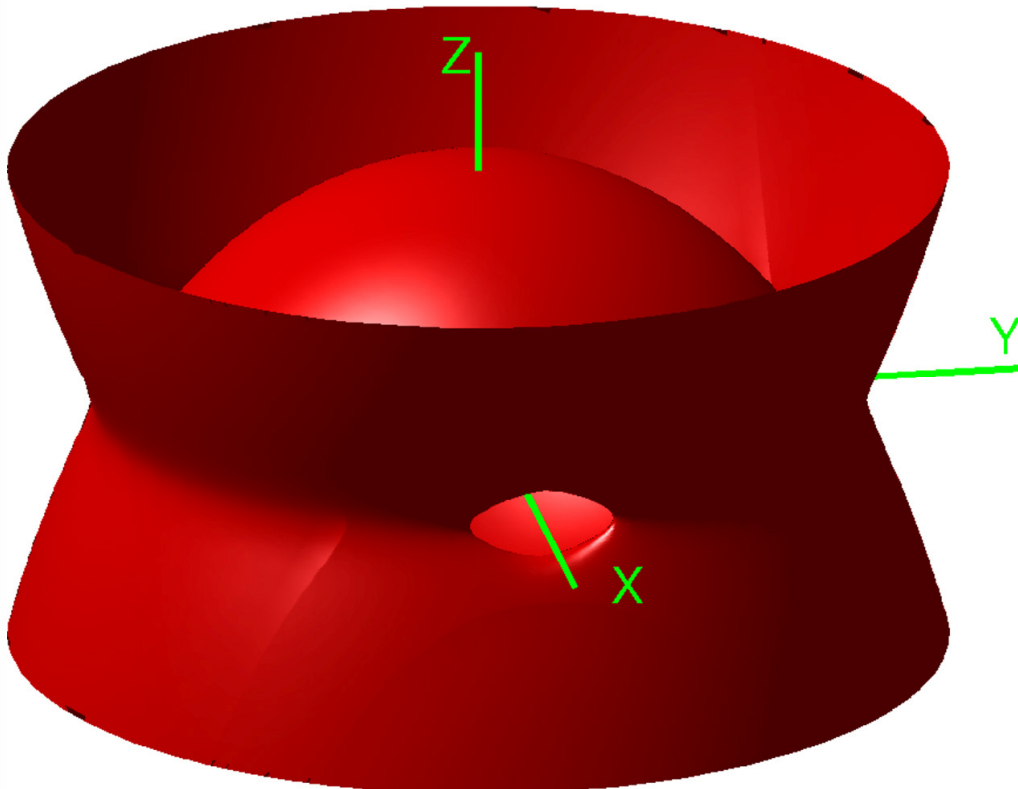


FIG. 2. Three-Dimensional Region of Exclusion for  $C = 3.0058$ .

3.0058. This value is characteristic of the largest member of the northern  $L_2$  halo family that appears in Fig. 1. Note that the interior region reflects motion *within* the center spheroid; the exterior region is defined as that space beyond the “pinched” cylindrical structure that surrounds the system; and, the TSC region is seen as the relatively small opening that connects the available regions of motion. A particle on or near the Sun-Jupiter line ( $x$ -axis), in the vicinity of the opening of the zero-velocity surface, can move across regions through this opening. The size of the opening narrows as the Jacobi Constant increases towards the value associated with the libration point  $L_2$ . Hence, only solutions associated with this range of Jacobi Constant values allow for transitions across regions similar to those experienced by Oterma and Helin Roman-Crockett. Also noted, the interior region is closed except for the single connection to the TSC region. Thus, the out-of-plane motion of a particle in the interior region remains bounded. The two comets in this study also exhibit bounded out-of-plane motion in the interior region. Observations based on numerical analysis indicate that, for trajectories that are propagated from initial conditions representing manifold surfaces, the out-of-plane excursion is loosely bounded by the  $A_z$  amplitude of the halo orbit from which they originate. Thus, by measuring the maximum out-of-plane excursion along the actual (ephemeris) path of the comet in the interior region, an initial guess for the  $A_z$  amplitude of a specific halo orbit is generated; this halo orbit is, then, likely to produce a trajectory arc that best matches the comet path.

#### *Stable and Unstable Manifolds Associated with a Periodic Orbit*

Given some initial observations concerning the search for trajectories that lie on manifold surfaces, that is, those associated with periodic halo orbits that may best match the comet paths, some additional relationships between the stable and unstable manifolds are notable. Consider a general nonlinear vector field,  $\dot{\mathbf{x}}(t) = \mathbf{f}(t, \mathbf{x}(t))$ . Suppose this vector field is linearized relative to a periodic solution,  $\mathbf{x}(t) = \mathbf{x}(t + T)$ . The linear system is described by  $\dot{\mathbf{y}}(t) = \mathbf{A}(t)\mathbf{y}(t)$ , where  $\mathbf{A}(t) = \mathbf{A}(t + T)$  and  $\mathbf{y}(t)$  is a perturbation from the periodic solution. Any solution to the variational equation can be represented in the following form,  $\mathbf{y}(t) = \Phi(t, t_0)\mathbf{y}(t_0)$  provided the state transition matrix satisfies the matrix differential equation  $\dot{\Phi}(t, t_0) = \mathbf{A}(t)\Phi(t, t_0)$ , with initial conditions  $\Phi(t_0, t_0) = I_n$  ( $I_n(i, i) = 1$  and  $I_n(i, j) = 0$  for  $i \neq j$ ). These equations must be satisfied for all time,  $t$ . Let  $\Delta t > 0$  and consider the following well-known variable transformation:  $\tau = -t$ ,  $\mathbf{y}(t) = \mathbf{G}\mathbf{z}(\tau)$  where  $\mathbf{G}$  represents a constant nonsingular matrix. For all the differential equations to be satisfied regardless of whether time flows forward,  $\Delta t > 0$ , or backwards,  $\Delta t < 0$ , the matrix  $\mathbf{G}$  must satisfy the following properties,  $\mathbf{G} = \mathbf{G}^{-1}$  but  $\mathbf{G} \neq I_n$ . For instance, the constant diagonal matrix with elements  $G(i, i) = (-1)^{i+1}$  satisfies both of these conditions. This requirement leads to a relationship between the state transition matrix in positive time ( $\Delta t > 0$ ), and the state transition matrix in negative time ( $\Delta t < 0 \Rightarrow \Delta \tau > 0$ ):  $\Phi(\tau, \tau_0) = \mathbf{G}^{-1}\Phi(t, t_0)\mathbf{G}$ . This result is crucial in establishing a relationship between the stable and unstable manifolds associated with a state on the periodic solution.

As previously mentioned, the stability of a periodic orbit can be assessed from the eigenvalues of the monodromy matrix,  $\Phi(T, 0)$ . Let  $\lambda_j$  denote the eigenvalues of  $\Phi(T, 0)$ , where  $j = 1, \dots, 6$ . Consider the eigenvalue problem  $\Phi(T, 0)\mathbf{v}_u = \lambda_u\mathbf{v}_u$  and  $\Phi(T, 0)\mathbf{v}_s = \lambda_s\mathbf{v}_s$ , where the subscript  $s$  again denotes stable and the subscript  $u$  denotes unstable quantities. The vectors  $\mathbf{v}_s$  and  $\mathbf{v}_u$  represent the corresponding stable and unstable eigenvectors associated with  $\lambda_s$  and  $\lambda_u$ , respectively. Since the

eigenvalues of the monodromy matrix appear as reciprocal pairs, let  $\lambda'_s = 1/\lambda_u$ . Through the application of the properties of the state transition matrix, the eigenvalue problem can be inverted and restated as  $\lambda'_s \mathbf{v}_u = \Phi(-T, 0) \mathbf{v}_u$ . From the time invariance property of the state transition matrix,  $\Phi(-T, 0) = G^{-1} \Phi(T, 0) G$ , it follows that  $\lambda'_s G \mathbf{v}_u = \Phi(T, 0) G \mathbf{v}_u$  and hence  $\mathbf{v}'_s = G \mathbf{v}_u$ , where the prime notation denotes negative time (i.e. numerical propagation with  $\Delta t < 0$ ). A similar approach reveals that  $\mathbf{v}'_s = G \mathbf{v}_u$ . This result, combined with the time invariance property of the state transition matrix, can be applied to the mapping  $\hat{\mathbf{Y}}^{w_u}(t_i) = \Phi(t_i, 0) \mathbf{v}_u / \|\Phi(t_i, 0) \mathbf{v}_u\|$  to establish a relationship between the unstable manifold in positive time ( $\hat{\mathbf{Y}}^{w_u}$ ), associated with the state  $\mathbf{x}(t_i)$  on the periodic orbit, and the unstable manifold in negative time ( $\hat{\mathbf{Y}}^{w_u}$ ), associated with the state  $\mathbf{x}(-t_i)$ :  $\hat{\mathbf{Y}}^{w_u}(t_i) = G \hat{\mathbf{Y}}^{w_u}(-t_i)$ . A similar relationship exists for the stable manifold ( $\hat{\mathbf{Y}}^{w_s}$ ) associated with  $\mathbf{x}(t_i)$  on the periodic orbit, that is,  $\hat{\mathbf{Y}}^{w_s}(t_i) = G \hat{\mathbf{Y}}^{w_s}(-t_i)$ . Consider the case of a simply symmetric periodic solution, such as a halo orbit. A halo orbit is symmetric about the  $xz$ -plane. Thus, if  $\mathbf{x}(t_i) = [x \ y \ z \ \dot{x} \ \dot{y} \ \dot{z}]^T$  represents a state on the halo orbit then  $\mathbf{x}(T - t_i) = [x \ -y \ z \ -\dot{x} \ \dot{y} \ -\dot{z}]^T$  also represents a state on the same orbit. Suppose that the nonlinear and linear systems are numerically propagated with  $\Delta t < 0$  and that the eigenvalue problem (in negative time) is solved to determine the stable and unstable eigenvectors associated with  $\Phi(-T, 0)$ . In negative time, a state on the unstable manifold asymptotically departs the periodic solution, locally. However, in real time,  $\Delta t > 0$ . Thus, the unstable manifold in negative time is, in reality, the stable manifold in positive time. That is, the unstable manifold associated with  $\mathbf{x}(-t_i)$  is also the stable manifold associated with  $\mathbf{x}(T - t_i)$ . This leads to the following relationships:  $\hat{\mathbf{Y}}^{w_s}(T - t_i) = G \hat{\mathbf{Y}}^{w_u}(t_i)$  and  $\hat{\mathbf{Y}}^{w_u}(T - t_i) = G \hat{\mathbf{Y}}^{w_s}(t_i)$ . That is, the stable manifold associated with the state  $\mathbf{x}(T - t_i)$  is a mirror image (about the  $xz$ -plane) of the unstable manifold associated with the state  $\mathbf{x}(t_i)$  on the same halo orbit. Similarly, the unstable manifold associated with the state  $\mathbf{x}(T - t_i)$  is a mirror image of the stable manifold associated with the state  $\mathbf{x}(t_i)$ . This fact further simplifies the search for a stable/unstable manifold trajectory that matches a segment along the path of a comet. Once the evolution of trajectories that represent the stable manifold originating from a particular halo family is well understood, then the behavior of the corresponding unstable manifold directly follows. Of course, this result is essentially an application of the symmetry due to time invariance (SP2).

Although SP1 and SP2 simplify the process of identifying a match, an initial guess is still not available. The search is generally initiated from the single observation that the matching trajectory that lies on the manifold surface is likely to originate from a halo orbit whose  $A_z$  amplitude is close to the maximum out-of-plane excursion of the comet in the interior region. Even if the initial search efforts are concentrated only on a northern family (by SP1) and only on the stable manifold associated with this family (by SP2), there are still two separate halo families to search, SJL1 and SJL2. Thus, a large solution space still exists. However, numerical analysis and extensive experience indicates that this initial choice is not critical. In order to establish this fact, it is necessary to introduce some notation to classify the available solutions.

## Numerical Results

### *Evolution of the Stable/Unstable Manifolds in the Sun-Jupiter System*

In order to characterize the evolution of a trajectory corresponding to a stable or unstable manifold associated with a particular halo family, and provide some struc-



ture to the search process, it is necessary to establish a set of parameters to identify (a) the desired halo orbit along the family, (b) the point of origin, that is, the fixed point,  $\mathbf{x}_e$ , along the orbit, and (c) the stable/unstable directions associated with  $\mathbf{x}_e$ . Since, as previously discussed, numerical results indicate that the out-of-plane excursion along a given trajectory that represents a manifold is loosely bounded by the  $A_z$  amplitude of the originating halo orbit, the  $A_z$  amplitude is used to parameterize the family. Clearly, as seen in Fig. 1, some members of the SJL1 (or SJL2) halo family share the same  $A_z$  amplitude. However, members of the halo family that constitute the subset most often producing matches for comet trajectory arcs all possess  $A_z$  amplitudes well below  $60 \times 10^6$  km. This fact is expected since neither OTR nor HRC exceed this value in terms of a maximum out-of-plane excursion. Thus, for this investigation, the  $A_z$  amplitude is an acceptable parameter. If the halo orbit is unstable, both a stable and an unstable manifold is associated with each state (fixed point) along the orbit. Thus, it is also necessary to characterize each state (fixed point) along a particular halo orbit. Figure 3 includes the  $yz$ -projection of an  $L_2$  northern halo orbit. Since the comets OTR and HRC possess a significant out-of-plane component, it is reasonable to characterize each point in the  $yz$ -projection of the halo orbit by its  $(y, z)$  coordinate. Note, however, that this particular parameterization is not as effective for smaller members of the halo family, that is, those close to the  $xy$ -plane. Nevertheless, the out-of-plane component of the position vector corresponding to either comet in this investigation is significant and, thus, the parameterization is still acceptable. To collapse the  $(y, z)$  pair into one parameter, let  $\alpha = \tan^{-1}(\sigma_1 y / \sigma_2 z)$  where  $\sigma_1$  is defined as  $+1$  for an  $L_1$  halo and  $-1$  for an  $L_2$  halo. The value of the integer  $\sigma_2$  equals  $+1$  for a northern halo and  $-1$  for a southern halo. This convention ensures that  $\alpha$  is always positive in the direction of motion along the orbit. Furthermore,  $\alpha$  is constrained to a range between  $0^\circ$  and  $360^\circ$ .

Consider the state characterized by the angle  $\alpha$  along a given halo orbit. Assume that the halo orbit is unstable such that there exist both stable and unstable directions associated with this state (fixed point) along the halo. The eigenvectors of the associated monodromy matrix,  $\Phi(T, 0)$ , are six-dimensional, with three position elements  $(x, y, z)$  and three velocity elements  $(v_x, v_y, v_z)$ . Thus, the six-dimensional unit stable and unstable eigenvectors,  $\hat{\mathbf{Y}}^{w/s/u}(t_i) = [x_{s/u} \ y_{s/u} \ z_{s/u} \ \dot{x}_{s/u} \ \dot{y}_{s/u} \ \dot{z}_{s/u}]^T$ , can each be expressed in terms of two three-dimensional vectors  $\mathbf{Y}_p^{w/s/u} = [x_{s/u} \ y_{s/u} \ z_{s/u}]^T$  and  $\mathbf{Y}_v^{w/s/u} = [\dot{x}_{s/u} \ \dot{y}_{s/u} \ \dot{z}_{s/u}]^T$ . Note that  $\mathbf{Y}_p^{w/s/u}$  and  $\mathbf{Y}_v^{w/s/u}$  are not themselves unit vectors. Since  $\mathbf{Y}_p^{w/s/u}$  and  $\mathbf{Y}_v^{w/s/u}$  are three-dimensional vectors, each can be represented in configuration space as an equivalent unit direction, relative to the Sun-Jupiter rotating frame, associated with the state  $\mathbf{x}(t_i)$  along the halo orbit. For instance, the unit vector along  $\mathbf{Y}_v^{w/s/u}(t_i)$  can be expressed in terms of azimuth relative to the rotating  $x$ -axis ( $\alpha_d$ ) and elevation relative to the  $xy$ -plane ( $\beta_d$ ). The azimuth is measured in the positive sense when  $\dot{y}_{s/u} > 0$ ; the elevation is measured in the positive sense when  $\dot{z}_{s/u} > 0$ . The azimuth angle ( $\alpha_d$ ) is constrained to be evaluated between  $\pm 180^\circ$  and the elevation angle ( $\beta_d$ ), then, always possesses a value between  $\pm 90^\circ$ . Each state, or fixed point, defined within a halo family—including all states along each orbit in that family—corresponds to a unique  $(\alpha_d, \beta_d)$  pair. The directional evolution of the vector  $\mathbf{Y}_v^{w/s/u}$  along the SJL2 halo family appears in Fig. 4. This figure includes contours of constant  $\alpha_d$  and  $\beta_d$  along sample members of the halo family. Contours of constant  $\alpha_d$  and  $\beta_d$  appear as nonlinear, smooth, three-dimensional curves along the halo family, while lines of constant  $\alpha$  are two-dimensional rays originating from  $(y, z) = (0, 0)$ . Numerical analysis indicates that the essential features of a collection of trajectories representing stable/unstable manifolds, associated with a particular

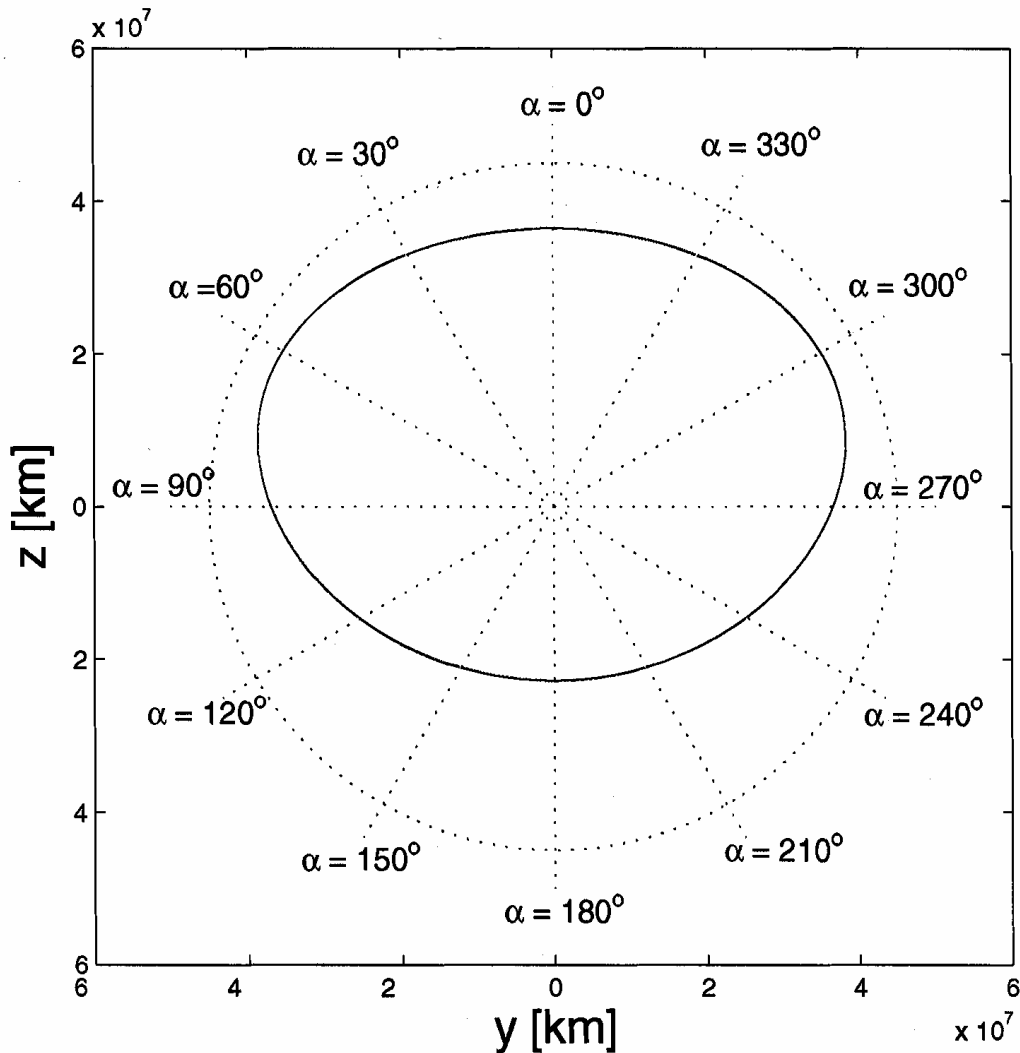


FIG. 3. Characterization of Fixed Points on a Northern  $L_2$  Halo Orbit.

halo family, are better preserved along lines of constant  $\alpha_d$  (azimuth), compared to lines of constant  $\alpha$  (angular location along the halo orbit) or lines of constant  $\beta_d$  (elevation). This numerically observed trend is illustrated in Fig. 5. This fact is most useful once a candidate match for a segment or arc along a particular comet trajectory is identified. Suppose a candidate match for the path of HRC in the TSC region is identified among the stable manifold trajectories associated with SJL2. HRC experiences several close approaches to Jupiter during TSC. If the flyby altitude of these close approaches is too low, one can improve the match—without losing the essential features—by selecting a neighboring trajectory with the same  $\alpha_d$ . Since the  $(\alpha_d, \beta_d)$  pairs are unique along a family, the new trajectory match—one that constitutes an improved match—is associated with a different member of SJL2.

#### *Numerical Near Symmetry of Solutions Across Halo Families*

Numerical observations on the evolution of the stable/unstable manifolds associated with SJL1, compared to the unstable/stable manifolds associated with SJL2, reveal some numerical near symmetries across halo families. In configuration space,

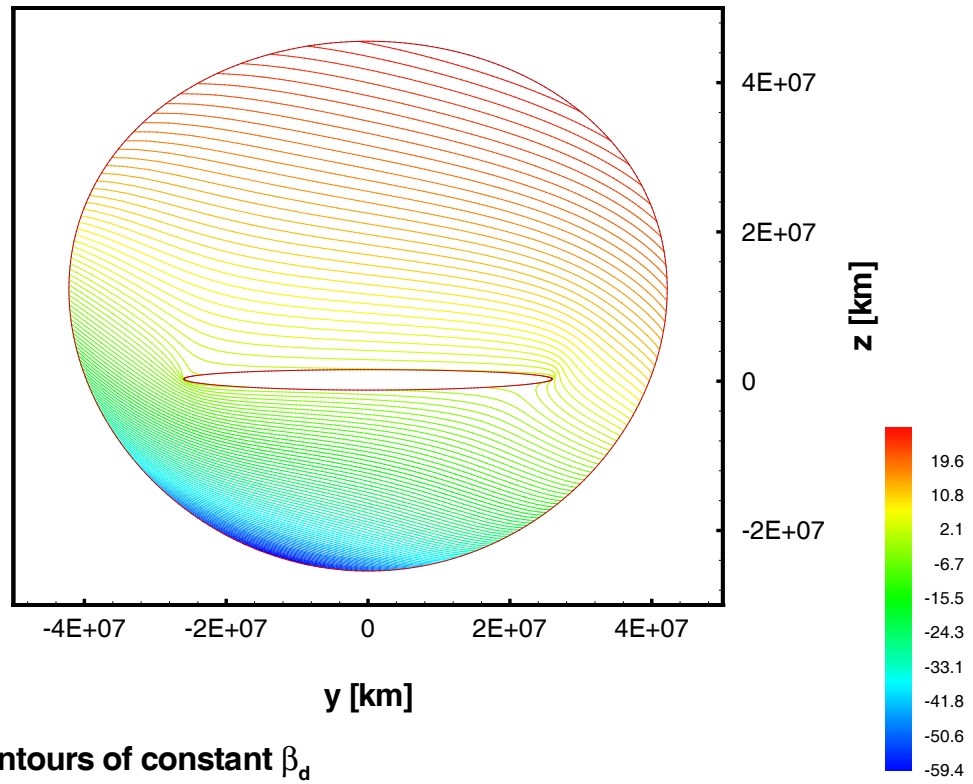
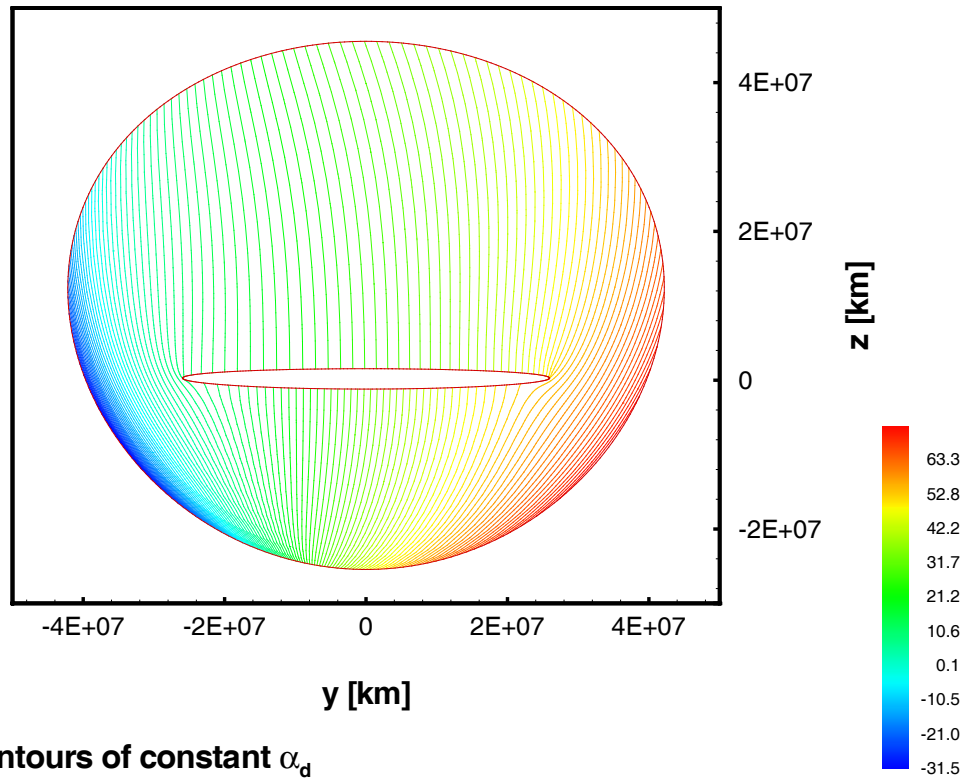


FIG. 4. Evolution of Stable Eigenvector Along SJL2.

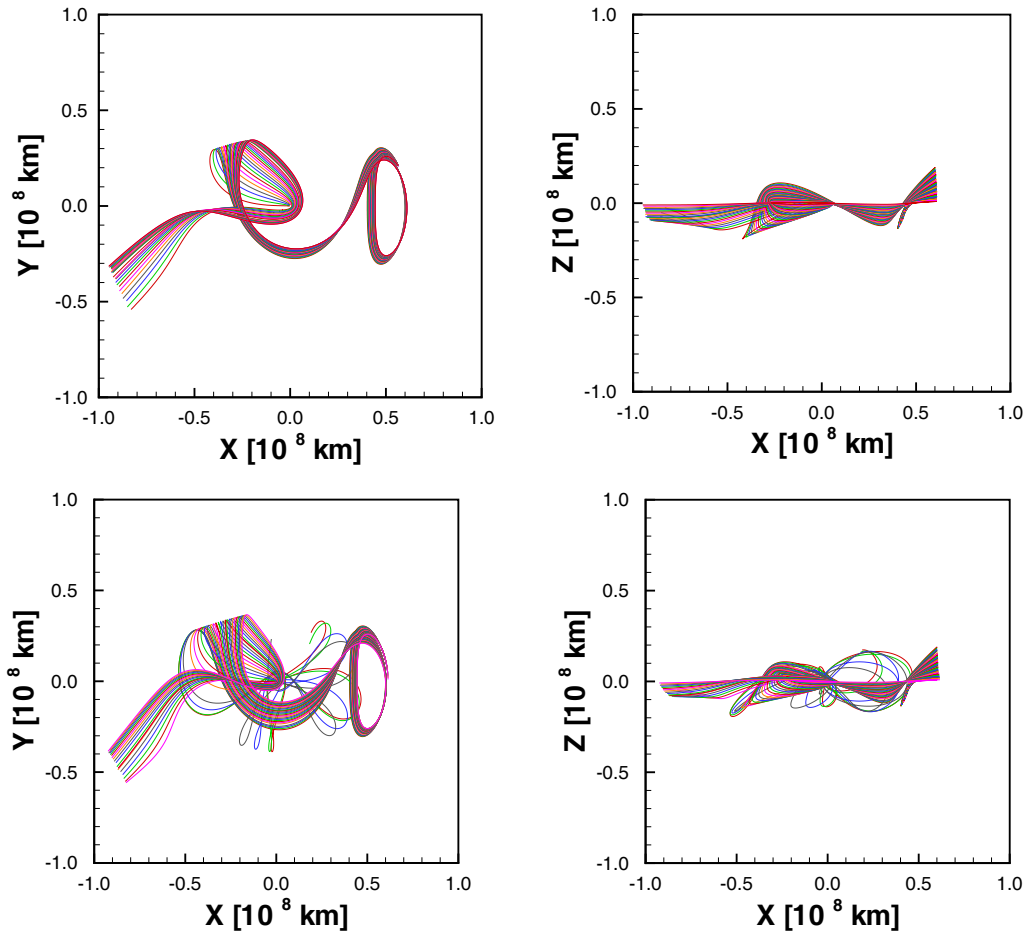
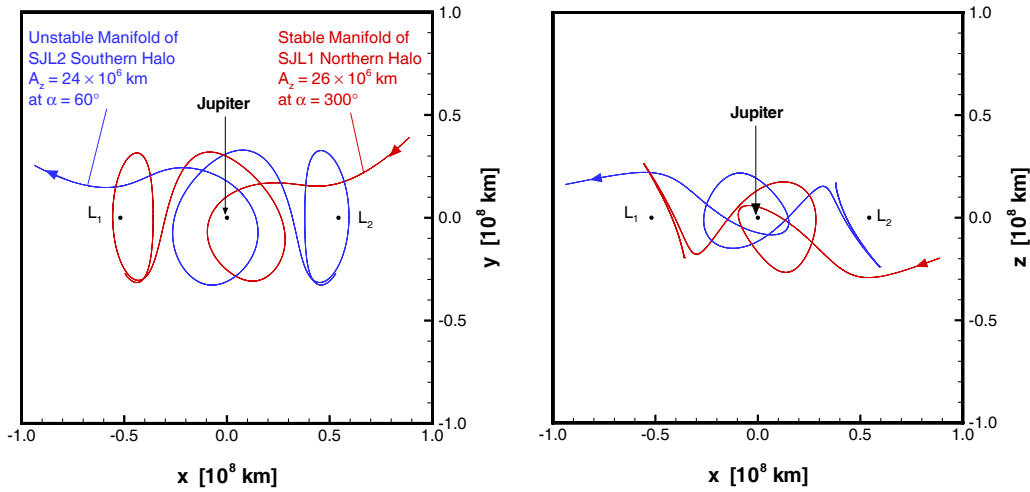


FIG. 5. Evolution of Stable Manifold Along  $\alpha_d = 43^\circ$  (top) and  $\alpha = 305^\circ$  (bottom).

particularly in the TSC region, a trajectory representing a stable manifold associated with the particular state  $\mathbf{x}(t_1) = [x_1 \ y_1 \ z_1 \ \dot{x}_1 \ \dot{y}_1 \ \dot{z}_1]^T$  along a northern  $L_1$  halo orbit shares many characteristics with the globalized unstable manifold associated with the alternate state vector  $\mathbf{x}(t_2) = [x_2 \ y_2 \ z_2 \ \dot{x}_2 \ \dot{y}_2 \ \dot{z}_2]^T$  along a southern  $L_2$  halo, when  $y_1 \approx y_2$ ,  $z_1 \approx -z_2$ . Note, that these coordinates correspond to the rotating frame typically defined in the CR3BP. These trajectories corresponding to the stable and unstable manifolds appear as near mirror images on the  $xy$ -plane (i.e., the plane of motion of the primaries) and their out-of-plane components are apparently inverted. This observation is illustrated in Fig. 6. The converse also appears valid for a southern  $L_1$  halo and a northern  $L_2$  halo, due to the natural  $xy$ -plane symmetry in the CR3BP (SP1). This numerically observed fact supports the conclusion that the initial choice of an  $L_1$  or an  $L_2$  halo orbit is arbitrary. Once a match, one that exhibits the most notable features of the comet trajectory in the TSC region, is identified, then the most appropriate halo family, that is,  $L_1$  or  $L_2$ , for the best match to the comet trajectory can be determined.

#### *Critical Energy Level for TSC*

In astronomy, the more commonly accepted definition of TSC requires only that the Joviocentric energy become negative at some instance during the comet's orbital evolution. However, the Joviocentric energy of a comet can become negative near



**FIG. 6.** Numerical Near Symmetry of Stable/Unstable Manifold Trajectories Across the SJL1 and SJL2 Halo Families.

Jupiter without forcing the comet to transition between regions. Thus, a more specific definition of TSC is implemented in this investigation. In any temporary satellite capture, the comet must first enter the TSC region as defined in terms of the zero-velocity surfaces. The comet will eventually exit the TSC region, but its heliocentric orbit will be affected by its encounter with Jupiter. The extent of this effect depends on the type of encounter. There are two possible types of encounters. Suppose the comet's path originates in the interior region. The simplest type of TSC (Type 1) occurs when the comet crosses into the TSC region and immediately exits to the exterior region. This type also applies to an immediate crossover from the exterior region to the interior region. A Type 1 capture is also defined as a fly-through of the TSC region. If, instead, the comet enters the TSC region and experiences more than one close encounter with Jupiter before it exits the TSC region, the encounter is defined as a Type 2.

Based on this definition for TSC, a specific energy level less than or equal to  $-2.5 \text{ km}^2/\text{s}^2$  is apparently required (in the CR3BP) for trajectories associated with SJL1 to experience a TSC. Along SJL1, trajectories generated to approximate the stable manifold, and that experience this crossover after one revolution in the interior region, are identified in Fig. 7 as a function of the critical angular location ( $\alpha$ ) and the  $A_z$  amplitude of the halo orbit. The shaded regions in Fig. 7 indicate the range over  $\alpha$  for which a trajectory defined along the stable manifold crosses into the TSC region from the interior region. This critical angle  $\alpha$  is crucial in identifying a match for OTR in the CR3BP. Recall that the search for a match is essentially the search for a "segment" of a trajectory arc (corresponding to a stable/unstable manifold) that reflects a segment of the comet's path, particularly during TSC. The TSC for OTR satisfies the conditions for a Type 1 capture, while that of HRC satisfies the conditions of a Type 2. Since neither OTR nor HRC ever evolve into a periodic halo orbit, it also becomes necessary to consider heteroclinic connections between the stable and unstable manifolds in the TSC region, or the long-term evolution of the stable or unstable manifolds, beyond the TSC stage. Thus, classification of the capture type before searching for a match is significant because the type of capture affects the structure of the search. That is, there are two directions in which a stable/unstable manifold can be propagated. One direction leads the trajectory into

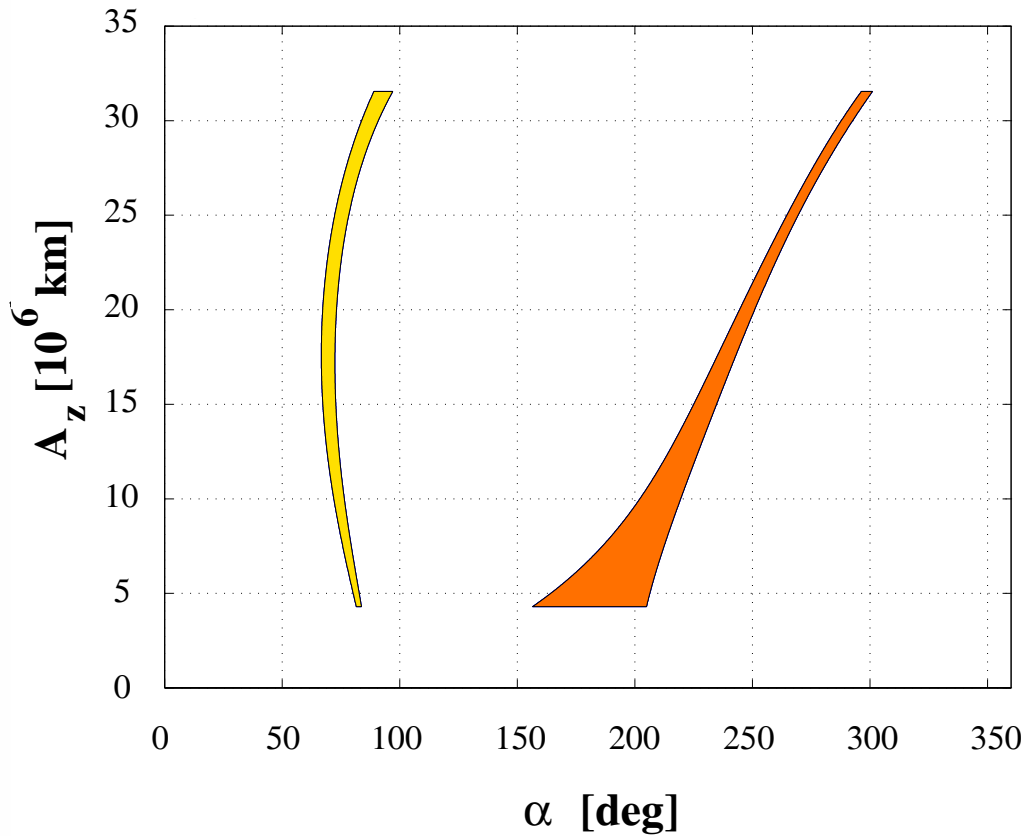


FIG. 7. Capture Condition for SJL1 Stable Manifold Trajectories After One Revolution in the Interior Region.

the TSC region, the other results in a trajectory that passes farther away from the TSC region. If a comet experiences a Type 1 capture, it is best to propagate the manifolds, i.e., numerically integrate the trajectories, away from the TSC region. If instead, the comet experiences a Type 2 capture, a good approximation for a match can be obtained by propagating the trajectories towards the TSC region and searching for heteroclinic connections between the stable and unstable manifolds [15, 23]. The difference is in the integration time. As illustrated in Fig. 7, if the trajectories representing the stable/unstable manifolds, associated with SJL1, are propagated towards the interior region, only a handful will return through the TSC region after one revolution. Certainly, the window of opportunity is wider as more revolutions are included. However, each revolution in the interior region adds to the integration time and degrades the accuracy of the solution. Furthermore, the analysis that led to Fig. 7 can be accomplished using the SJL2 family instead, by propagating the stable/unstable manifolds towards the exterior region. However, since the exterior region is open, and beyond the heliocentric orbit of Jupiter, the return time to the opening of the zero-velocity surface is much longer than the return time for SJL1 trajectories, which further increases the numerical integration error.

#### *Identification of a Match for Oterma*

In the past, OTR was captured by Jupiter on two separate occasions; once from 1935 to 1939, and later on from 1962 to 1964. Both encounters with Jupiter resulted in a Type 1 TSC. The search for a match to reflect these flythroughs begins by mea-

asuring the maximum out-of-plane excursion of the comet path while it orbits the Sun in the interior region. Based on this maximum out-of-plane excursion, an initial guess for the  $A_z$  amplitude of the halo orbit can be obtained. From the plot in Fig. 7, states along this halo orbit can be determined that will result in a trajectory along the stable manifold that returns through the opening of the zero-velocity surface after one revolution in the interior region. If a candidate match is identified, but the direction is inverted, or the trajectory itself appears inverted, the symmetry properties (SP1 and SP2) can be applied to improve the match for a given  $A_z$  amplitude. If, for the initial  $A_z$  amplitude, a candidate match exists but is not sufficiently close to the path of the comet, the features of the trajectory can be adjusted by examining nearby trajectories along lines of constant  $\alpha_d$ . Thus, the essential characteristics of the trajectory will be preserved by changing the  $A_z$  amplitude of the halo orbit, while maintaining the azimuth of the stable (or unstable) eigenvectors in a constant direction. The best match obtained in the CR3BP can be further improved by transferring the solution into the ephemeris model. In the ephemeris model, periodic halo orbits do not exist. Thus, transferring the orbit into this model requires its transformation into a quasi-periodic Lissajous trajectory. The transfer is accomplished by

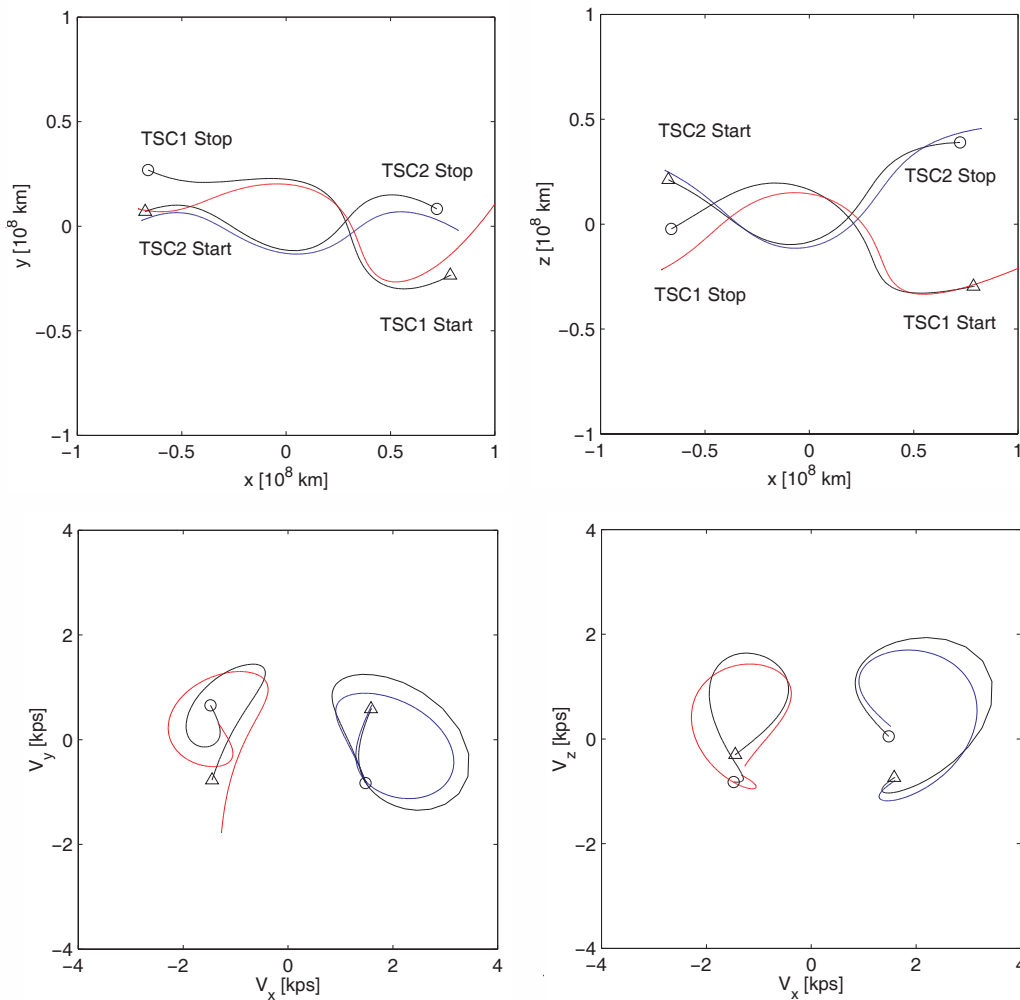
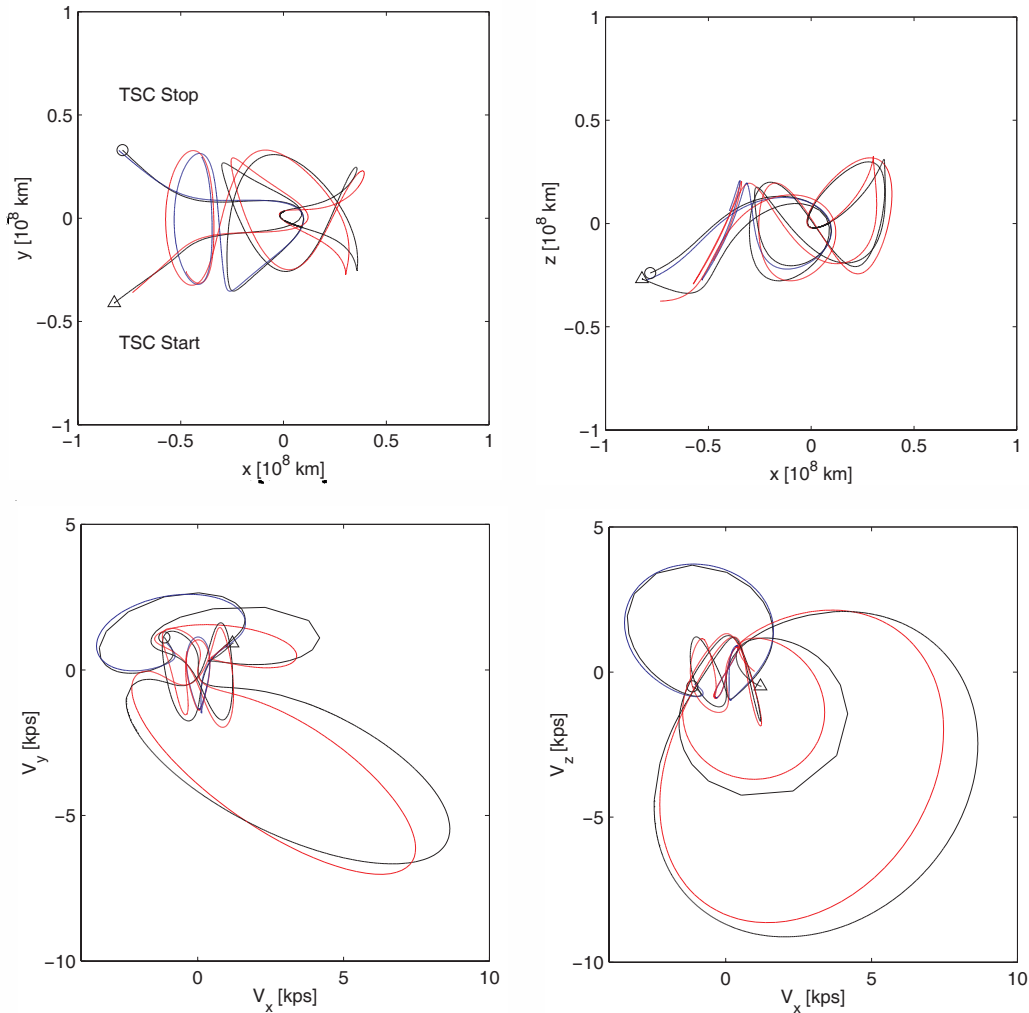


FIG. 8. Position and Velocity Match for Oterma in the Ephemeris Model (1935-1939 & 1962-1964).

selecting several target points along the original halo orbit as an initial guess for the quasi-periodic solution in the ephemeris model and applying a differential corrections process [25–27] for multiple revolutions to obtain a Lissajous trajectory that is similar to the original halo orbit. Once the orbit is transferred into the ephemeris model, it is necessary to reestablish the comet match. The numerical approximation of stable and unstable manifolds associated with quasi-periodic orbits is based on the power method discussed by G. Gómez, A. Jorba, J. Masdemont, and C. Simó [28]. Though the matching trajectory (or trajectory arc) in the ephemeris model will not originate from the same angular location ( $\alpha$ ), it will be in the neighborhood of the original value. The match for OTR as it is developed and computed in the ephemeris model is plotted in Fig. 8. The red curve in this figure represents the stable manifold associated with a northern SJI1 quasi-periodic Lissajous trajectory computed in the ephemeris model. The black curve represents a segment along the comet's orbital path available directly from comet ephemeris data.



**FIG. 9.** Position and Velocity Match for Helin-Roman-Crockett in the Ephemeris Model (1966-1985).



*Identification of a Match for Helin-Roman-Crockett*

HRC experienced a Type 2 capture by Jupiter from 1966 until 1985. Since HRC remained in the vicinity of Jupiter for an extended period of time, the search for a match is simplified by considering possible heteroclinic connections between the stable and unstable manifolds associated with SJL1 and SJL2. The search process is the same as that used for OTR, except that, in this case, the near symmetry across halo families offers an advantage in establishing a match. In this case, the match for HRC is a combination of the stable and unstable manifolds associated with a southern SJL1 halo. Both the trajectories, that is, one each corresponding to the stable and the unstable manifolds, respectively, originate from the same halo orbit and, hence, share the same Jacobi Constant. Once again, to improve the accuracy of the match, the trajectories are transferred from the CR3BP into the ephemeris model. The match, as computed in the ephemeris model, is plotted in Fig. 9. The red curve represents a segment along the stable manifold for a southern SJL1 quasi-periodic Lissajous trajectory. The unstable manifold appears as a blue curve for the same SJL1 Lissajous trajectory. The orbital path of the HRC comet is directly plotted from ephemeris data as a black curve.

**Conclusion**

The natural symmetries in the CR3BP and the observed near-symmetries between the  $L_1$  and  $L_2$  halo families—based on numerical analysis—provide the basic understanding necessary to begin the search process and ultimately identify a match in the CR3BP, for a particular Jupiter family short-period comet. A dynamical systems perspective has provided significant insight into the geometry of solutions in the Sun-Jupiter system and offered a simple model to account for the most notable features of the TSC phenomena observed in Jupiter family short-period comets. Furthermore, the fact that the observed motion of these comets can be explained in the context of dynamical systems suggests further applications to the motion of natural bodies in the solar system. This dynamical insight also extends to potential applications in support of interplanetary mission design for spacecraft. The next step in this investigation is to apply this modeling approach to the capture of other short-period Jupiter family comets, such as Gehrels 3. Although the search strategy discussed here has been successfully applied to the capture motion of HRC and OTR, a slightly different approach might be necessary in modeling other Jupiter family comets. Since the *three*-dimensional, chaotic nature of TSC results in distinct types of motion during capture, modeling other comets might require consideration of the stable and unstable manifold solutions associated with other types of periodic orbits in the Sun-Jupiter system, aside from the SJL1 and SJL2 halo families. Furthermore, comets such as Gehrels 3 that experience low altitude approaches to Jupiter might also require a more complex model that incorporates additional perturbing forces. Nevertheless, the modeling of the TSC phenomena has generated additional understanding of the natural dynamics in this R3BP regime.

**Acknowledgments**

This research was carried out at Purdue University and at the Jet Propulsion Laboratory, California Institute of Technology, under a contract with the National Aeronautics and Space Administration.

## References

- [1] 39P/OTERMA. Available at: <http://www.comets.amsmeteors.org/comets/pcomets/039p.html>, April 27<sup>th</sup>, 1995.
- [2] KAZIMIRCHAK-POLONSKAYA, E. I. "The Major Planets as Powerful Transformers of Cometary Orbits," *The Motion, Evolution of Orbits, and Origin of Comets*, International Astronomical Union: Symposium No. 45, 1972, pp. 373–397.
- [3] CARUSI, A. and POZZI, F. "Planetary Close Encounters Between Jupiter and About 3000 Fictitious Minor Bodies," *The Moon and the Planets*, Holland: D. Reidel Publishing Company, 1978, Vol. 19, pp. 71–87.
- [4] CARUSI, A. and VALSECCHI, G. B. "Numerical Simulations of Close Encounters Between Jupiter and Minor Bodies," *Asteroids*, Edited by Tom Gehrels, The University of Arizona Press, 1979, pp. 391–415.
- [5] CARUSI, A. and VALSECCHI, G. B. "Planetary Close Encounters: Importance of Nearly Tangent Orbits," *The Moon and the Planets*, Holland: D. Reidel Publishing Company, 1980, Vol. 22, pp. 113–124.
- [6] CARUSI, A. and VALSECCHI, G. B. "Temporary Satellite Captures of Comets by Jupiter," *Astronomy and Astrophysics*, Vol. 94, 1981, pp. 226–228.
- [7] CARUSI, A., KRESÁK, L., and VALSECCHI, G. B. "Perturbations by Jupiter of a Chain of Objects Moving in the Orbit of Comet Oterma," *Astronomy and Astrophysics*, Vol. 99, 1981, pp. 262–269.
- [8] CARUSI, A., PEROZZI, E., and VALSECCHI, G. B. "Low Velocity Encounters of Minor Bodies with the Outer Planets," *Dynamical Trapping and Evolution in the Solar System*, Holland: D. Reidel Publishing Company, 1983, pp. 377–395.
- [9] CARUSI, A., KRESÁK, L., PEROZZI, E., and VALSECCHI, G. B. "First Results of the Integration of Motion of Short-Period Comets Over 800 Years," *Dynamics of Comets: Their Origin and Evolution*—Edited by A. Carusi and G. B. Valsecchi, Holland: D. Reidel Publishing Company, 1985, pp. 319–340.
- [10] CARUSI, A. and VALSECCHI, G. B. "Dynamics of Comets," *Chaos, Resonance, and Collective Dynamical Phenomena in the Solar System—Proceedings of the 152<sup>nd</sup> Symposium of the International Astronomical Union*, July 15–19, 1991, pp. 255–268.
- [11] HORED T, G. P. "Capture of Planetary Satellites," *The Astronomical Journal*, Vol. 81, No. 8, August 1976, pp. 675–678.
- [12] HEPPE NHEIMER, T. A. "On the Presumed Capture Origin of Jupiter's Outer Satellites," *Icarus*, Vol. 24, 1975, pp. 172–180.
- [13] HEPPE NHEIMER, T. A. and PORCO, C. "New Contributions to the Problem of Capture," *Icarus*, Vol. 30, 1977, pp. 385–401.
- [14] LO, M. W. and ROSS, S. D. "SURFing the Solar System: Invariant Manifolds and the Dynamics of the Solar System," JPL IOM 312/97, 2–4, 1997.
- [15] KOON, W. S., LO, M. W., MARSDEN, J. E., and ROSS, S. D. "Heteroclinic Connections Between Periodic Orbits and Resonance Transitions in Celestial Mechanics," presented to the Society for Industrial and Applied Mathematics (SIAM), Snowbird, Utah, May 1999.
- [16] WIGGINS, S. *Introduction to Applied Nonlinear Dynamical Systems and Chaos*, New York: Springer-Verlag, 1990.
- [17] GUCKENHEIMER, J. and HOLMES, P. *Nonlinear Oscillations, Dynamical Systems, and Bifurcations of Vector Fields*, New York: Springer-Verlag, 1983.
- [18] NAYFEH, A. H. and MOOK, D. T. *Nonlinear Oscillations*, New York: John Wiley and Sons, 1995.
- [19] PERKO, L. *Differential Equations and Dynamical Systems*, New York: Springer-Verlag, 1996.
- [20] HALE, J. K. and KOÇAK, H. *Dynamics and Bifurcations*, New York: Springer-Verlag, 1991.
- [21] NAYFEH, A. H. and BALACHANDRAN, B. *Applied Nonlinear Dynamics*, New York: John Wiley and Sons, 1995.
- [22] KHALIL, H. K. *Nonlinear Systems*, New Jersey: Prentice Hall, 1996.
- [23] PARKER, T. S. and CHUA, L. O. *Practical Numerical Algorithms for Chaotic Systems*, New York: Springer-Verlag, 1989.
- [24] SZEBEHELY, V. *Theory of Orbits: The Restricted Problem of Three Bodies*, New York: Academic Press, 1967.

- [25] HOWELL, K. C. and PERNICKA, H. J. "Numerical Determination of Lissajous Trajectories in the Restricted Three-Body Problem," *Celestial Mechanics*, Vol. 41, 1988, pp. 107-124.
- [26] HOWELL, K. C., MAINS, D. L., and BARDEN, B. T. "Transfer Trajectories from Earth Parking Orbits to Sun-Earth Halo Orbits," AAS Paper 94-160, AAS/AIAA Spaceflight Mechanics Conference, Cocoa Beach, Florida, February 14-16, 1994.
- [27] HOWELL, K. C., BARDEN, B. T., and WILSON, R. S. "Trajectory Design Using a Dynamical Systems Approach with Applications to GENESIS," AAS Paper 97-709, AAS/AIAA Astrodynamics Specialists Conference, Sun Valley, Idaho, August 4-7, 1997.
- [28] GÓMEZ, G., JORBA, A., MASDEMONT, J., and SIMÓ, C. "Final Report: Study Refinement of Semi-Analytical Halo Orbit Theory," ESOC Contract Report, Technical Report 8625/89/D/MD(SC), Barcelona, Spain, April 1991.